**1733+5533**

The sightline towards the quasar Q1733+5533 ($V = 18.0$, $z_{em} = 1.072$) contains a DLA system at $z_{abs} = 0.9981$ with a column density of log N(HI) $= 20.70^{+0.04}_{-0.03}$ cm$^{-2}$ (RTN06). A complete optical data set, and $H$ and $K$ band data exist for this field.

**Three $\sigma$ surface brightness limits and seeing measurements** for these observations are given. These limits indicate that a galaxy with diameter $d = 10$ kpc, as faint as $L_{u'} = 0.05L^{\star}_{u'}$, $L_{g'} = 0.02L^{\star}_{g'}$, $L_{r'} = 0.02L^{\star}_{r'}$, $L_H = 0.14L^{\star}_H$, $L_K = 0.22L^{\star}_K$ can be detected at the absorber redshift.

**Images:**
$30'' \times 30''$ $u', g', r', i', H, K$ images are shown. North is up and east is to the left. The images correspond to $\approx 240 \times 240$ kpc$^2$ at the absorber redshift. The quasar PSF subtraction residuals have been masked in the optical images, and the position of its centre is marked by a "+".

**Photo-z's:**
Photometric redshifts could not be determined for any of the objects in this field, since they are all detected in fewer than four bands. Although the $H$-band detection of Object 1 is of low significance, its $g' - H = 1.54$ color is consistent with it being a late type galaxy (Im) at $z_{abs}$. It is selected as the absorber along this sightline. The $g' - r'$ color of Object 3 is highly uncertain and does not constrain its redshift.

Table 1: $3\sigma$ Surface Brightness Limits ($\mu$) and Seeing Measurements ($\Theta$)

| Q1733+5533 | | | | | | | | | | | | | |
|---|---|---|---|---|---|---|---|---|---|---|---|---|---|
| $\mu_{u'}$ | $\mu_{g'}$ | $\mu_{r'}$ | $\mu_{i'}$ | $\mu_J$ | $\mu_H$ | $\mu_K$ | $\Theta_{u'}$ | $\Theta_{g'}$ | $\Theta_{r'}$ | $\Theta_{i'}$ | $\Theta_J$ | $\Theta_H$ | $\Theta_K$ |
| (mags/arcsec$^2$) | | | | | | | (arcsec) | | | | | | |
| 26.5 | 25.9 | 24.7 | 24.2 | $\cdots$ | 22.4 | 21.9 | 1.2 | 1.6 | 1.4 | 0.9 | $\cdots$ | 1.1 | 0.9 |

Table 2: Q1733+5533 Infrared Photometry

| Q1733+5533 $z_{abs} = 0.9981$ | | | | | | | | | |
|---|---|---|---|---|---|---|---|---|---|
| Object | $\Delta\alpha$[a] $''$ | $\Delta\delta$[a] $''$ | $\theta$[a] $''$ | $J \pm \sigma_J$ | DS ($N_{pix}$)[b] | $H \pm \sigma_H$ | DS ($N_{pix}$)[b] | $K \pm \sigma_K$ | DS ($N_{pix}$)[b] |
| QSO | 0.0 | 0.0 | 0.0 | $\cdots$ | $\cdots$ | 17.93 ± 0.01 | 17.3 (110) | 17.70 ± 0.01 | 16.4 (98) |
| 1 | −7.1 | −4.5 | 8.4 | $\cdots$ | $\cdots$ | 22.85 ± 0.19 | 1.9 (11) | $\cdots$ | $\cdots$ |
| 2 | +1.5 | −11.6 | 11.7 | $\cdots$ | $\cdots$ | $\cdots$ | $\cdots$ | $\cdots$ | $\cdots$ |
| 3 | −1.0 | −11.9 | 12.0 | $\cdots$ | $\cdots$ | $\cdots$ | $\cdots$ | $\cdots$ | $\cdots$ |

[a] Relative to the QSO.

[b] $N_{pix}$ is the number of pixels within the detection isophote.

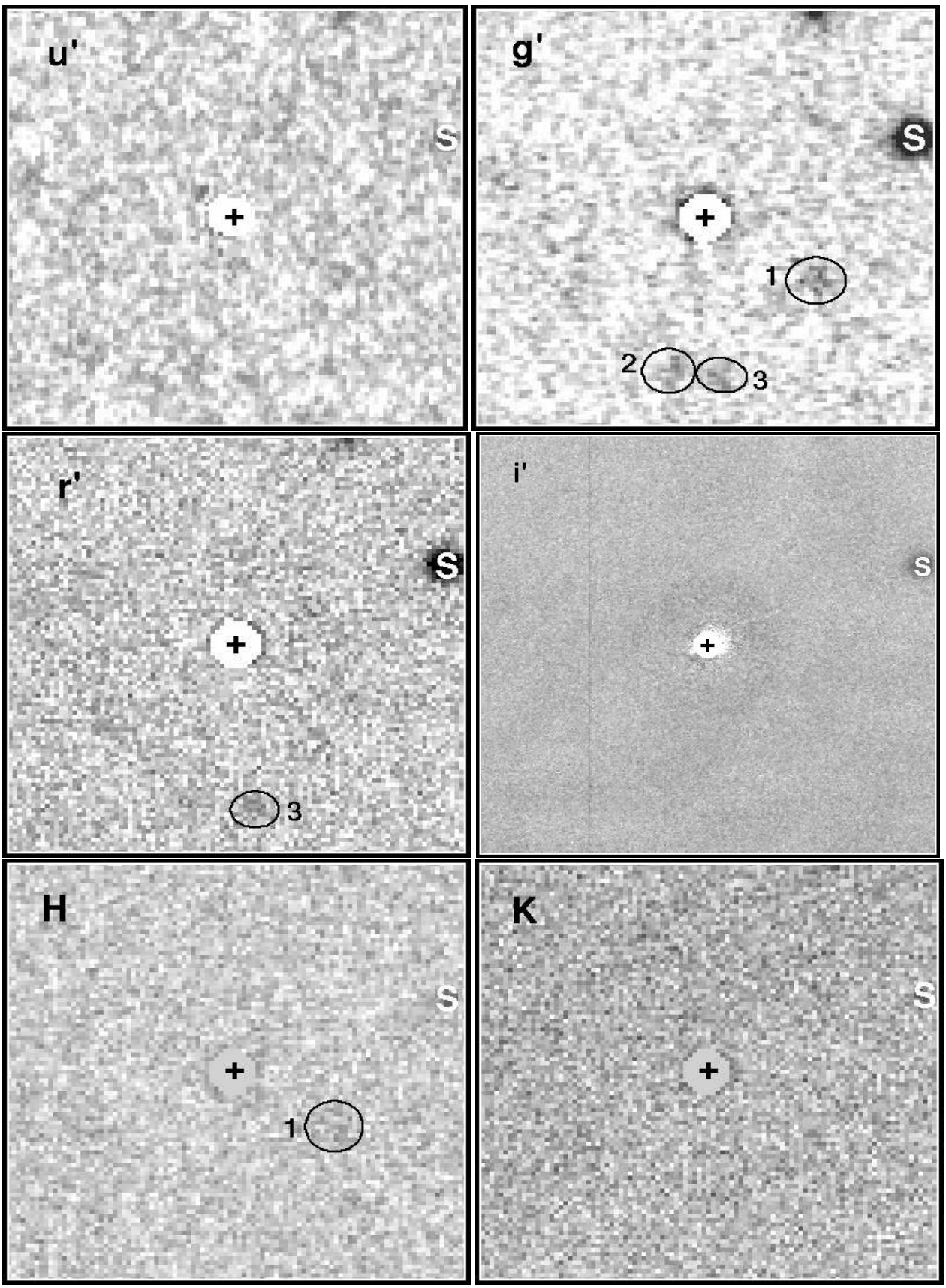
u'
S
+
g'
S
+
1
2
3
r'
S
+
3
i'
S
+
H
S
+
1
K
S
+

Table 3: Q1733+5533 Optical Photometry

| Q1733+5533 $z_{abs} = 0.9981$ | | | | | | | | | | | |
|---|---|---|---|---|---|---|---|---|---|---|---|
| Object | $\Delta\alpha^{a}$ $''$ | $\Delta\delta^{a}$ $''$ | $\theta^{a}$ $''$ | $u' \pm \sigma_{u'}$ | DS $(N_{pix})^{b}$ | $g' \pm \sigma_{g'}$ | DS $(N_{pix})^{b}$ | $r' \pm \sigma_{r'}$ | DS $(N_{pix})^{b}$ | $i' \pm \sigma_{i'}$ | DS $(N_{pix})^{b}$ |
| QSO | 0.0 | 0.0 | 0.0 | 18.89 ± 0.20 | 48.2 (513) | 17.83 ± 0.05 | 54.4 (829) | 17.91 ± 0.04 | 35.0 (486) | 18.11 ± 0.11 | 20.9 (2527) |
| 1 | −7.1 | −4.5 | 8.4 | ··· | ··· | 24.39 ± 0.30 | 2.9 (37) | ··· | ··· | ··· | ··· |
| 2 | +1.5 | −11.6 | 11.7 | ··· | ··· | 25.10 ± 0.49 | 2.0 (27) | ··· | ··· | ··· | ··· |
| 3 | −1.0 | −11.9 | 12.0 | ··· | ··· | 25.24 ± 0.54 | 2.0 (24) | 25.23 ± 0.91 | 1.5 (11) | ··· | ··· |

[a] Relative to the QSO.

[b] $N_{pix}$ is the number of pixels within the detection isophote.